Nanotechnology for Environmental Engineering (2021) 6:27
https://doi.org/10.1007/s41204-021-00122-3

ORIGINAL PAPER

Temperature effect on phosphogypsum conversion into potassium fertilizer K_2SO_4 and portlandite

Ilham Zdah[1] · Hanan El Alaoui-Belghiti[1] · Ayoub Cherrat[1] · Yassine Ennaciri[1] · Rachid Brahmi[2] · Mohammed Bettach[1]

Received: 24 February 2021 / Accepted: 29 April 2021 / Published online: 14 May 2021

Abstract
Phosphogypsum (PG) waste causes several environmental problems. The present work proposes an attractive process to recycle this industrial waste via the wet conversion and contributes to solve this problem. In our previous work, we tried to convert the PG by KOH at ambient temperature, but its total conversion was limited at the concentration of 0.6 M which requires a high cost to recrystallize K_2SO_4 from the filtrate. Therefore, to avoid the formation of syngenite (parasitic phase) and to increase the PG reactivity, we have varied the temperature parameter in this work. The experiments are performed with stoichiometric proportions. According to experimental results, optimal reaction conditions are obtained at 80 °C during one hour and permitted having two valuable products: $Ca(OH)_2$ as precipitate and high concentrated K_2SO_4 solution. These products find their applications in several industrial fields. In order to prove their quality, the complete PG decomposition is evidenced by X-ray diffraction and Fourier transform infrared spectroscopy. Thermogravimetric analysis combined to mass spectrometry measurements shows the partial carbonation of the portlandite into calcite and allows there quantification. Scanning electron microscopy images reveals two different types of grain shape in the precipitate. Economical and numerical approach permits to calculate the benefit of about 500 $ per ton of PG converted in addition the resolution of a serious environmental problem.

Keywords Phosphogypsum · Portlandite $Ca(OH)_2$ · Potassium fertilizer K_2SO_4 · Valorization · Temperature effect

Introduction

The phosphoric acid manufacture by the wet process produces high quantities of phosphogypsum (PG) waste. About 15 million tons are produced in Morocco, this quantity will increase in the coming years. PG is commonly stored in heap or dumped in the Atlantic Ocean [1, 2]. It has a negative impact on the environment and human health. Some authors have proposed solutions to recover or to reuse this waste in several fields, for example in agriculture as soil improvement and fertilization or in alkaline biochar production processing acidic PG waste [3, 4]. In cement, PG delay the setting time of the cement, which allows it to replace the natural gypsum in the cement and brick industry [5–9]. In plaster and cement industry, after appropriate treatment with sulfuric acid, PG meets standards that limit P_2O_5 and F impurities for its use as alternative to natural gypsum [10].

Other researchers have worked on the valuation of PG by converting it with an alkali fluoride (NaF) or ammonia and hydrofluoric acid according to the following reactions [11, 12]:

$$CaSO_4 \cdot 2H_2O + 2NaF \rightarrow CaF_2 + Na_2SO_4 + 2H_2O \quad (1)$$

$$CaSO_4 \cdot 2H_2O + NH_3 + 2HF \rightarrow CaF_2 + (NH_4)HSO_4 + 2H_2O \quad (2)$$

The valorization of PG by alkaline carbonates (K_2CO_3, Na_2CO_3 and Li_2CO_3) have also been studied, its conversion yields to marketable products, as explained in the following reactions [13, 14]

$$CaSO_4 \cdot 2H_2O + K_2CO_3 \rightarrow K_2CO_3 + K_2SO_4 + 2H_2O \quad (3)$$

✉ Hanan El Alaoui-Belghiti
belghitihanan@gmail.com

[1] Laboratory of Physical Chemistry of Materials (LPCM), Faculty of Science, El Jadida, Chemistry, El Jadida, Morocco

[2] Laboratory of Coordination and Analytical Chemistry (LCCA), Faculty of Science, El Jadida, Chemistry, El Jadida, Morocco

$$CaSO_4 \cdot 2H_2O + Na_2CO_3 \rightarrow Na_2CO_3 + K_2SO_4 + 2H_2O \quad (4)$$

$$CaSO_4 \cdot 2H_2O + Li_2CO_3 \rightarrow Li_2CO_3 + K_2SO_4 + 2H_2O \quad (5)$$

Other works used alkaline hydroxide (NaOH) to convert PG. The reaction is expressed as the following [15]:

$$CaSO_4 \cdot 2H_2O + NaOH \rightarrow Na_2SO_4 + K_2SO_4 + 2H_2O \quad (6)$$

In these wet conversions. PG is used as raw material for chemical processes. Cited reactions were carried out at room temperature and atmospheric pressure. Specific conditions must be controlled to improve product quality like the attack duration and initial reagents concentrations to avoid syngenite ($K_2Ca(SO_4)_2{\cdot}2H_2O$) formation. Nevertheless, valued quantity of PG remains lower compared to that produced.

Potassium sulfate K_2SO_4 is produced from different natural ores such as Kainite $KCl{\cdot}MgSO_4{\cdot}3H_2O$ or Leonite $K_2SO_4{\cdot}MgSO4{\cdot}4H_2O$. It can be also synthetized according to the Mannheim process where the reaction between H_2SO_4 acid and KCl requires a temperature of 800 °C [16]. Other researchers produced K_2SO_4 from gypsum, ammonia and KCl in aqueous solution, but chloride content in the final product avoid its use in agriculture [17, 18].

The present work suggests an attractive process allowing total PG conversion by potassium hydroxide KOH. This decomposition leads to potassium sulfate K_2SO_4 and calcium hydroxide $Ca(OH)_2$ formation. K_2SO_4 is used as a fertilizer; growers frequently use it for crops where chlorides additions should be avoided. In such cases, K_2SO_4 makes a very suitable K and S source, whereas $Ca(OH)_2$ is a source of CaO which is the main component of Portland cement manufacturing. Its use in cement makes it possible to control the hydration mechanism of the cement and provides information on the duration of the pozzolanic reaction [19]. It has also been used as adsorbent for radioactive and heavy elements in wastewater, desulfurizing agent and material for thermal energy storage [20, 21]. In addition, mineral carbonation is a mitigation strategy to reduce global anthropogenic CO_2 emissions, which is constantly increasing [22–24].

Our previous work studied the PG conversion by KOH at several concentrations and various durations, but this reaction was limited at the concentration 0.6 M of PG due to the formation of parasitic phase of syngenite [25].

The proposal discussed in this work is to defy this problem by studying temperature effect on reaction progression especially in a saturated medium and therefore on the quality of obtained products by spending lesser energy compared to other processes. Indeed, diluted filtrates require a lot of energy to recrystallize the salt. This process have also other advantages, it is ecological and enhances a significant environmental benefit that allows the PG conversion, which is otherwise considered as hazardous waste. In addition, it is not difficult and not expensive, In fact, 1 ton of PG react with 0,651 ton of KOH (600 $ per ton [26]) to produce 0.430 ton of portlandite (420 $ per ton [26]) and 1.013 ton of K_2SO_4 (700 $ per ton [26]). This economical approach permits to benefit of about 500 $ per ton of PG converted, which can largely cover transport cost and the energy used during this process and does not require any difficult operation for recuperating these valuables products.

Material and methods

Phosphogypsum was taken from the fertilizer plant Morocco Phosphorus, located at twenty kilometers from the town of El Jadida. This phosphogypsum was washed to serve as a raw material for all tests. The washing step serves to remove soluble impurities as well as several organic matters in suspension. The potassium hydroxide KOH used in this research was from Fluka, with the purity ≥ 85%.

For each reaction, the mass corresponding to the desired concentration is dissolved in the potassium hydroxide solution of well-known concentration. The reaction is displaced in the direction of K_2SO_4 and $Ca(OH)_2$ formations. This is because portlandite $Ca(OH)_2$ ($Kps = 7.9 \times 10^{-6}$ at 25 °C) is less soluble than PG ($Kps = 3.14 \times 10^{-5}$ at 25 °C). The mixtures were put under stirring during one hour. A white precipitates $Ca(OH)_2$ are formed. They are separated from the solution by simple filtration and afterward dried in an oven at 60° C. The filtrates, which contain K_2SO_4 are placed in the oven at 60 °C to recrystallize the salts (Fig. 1). All compounds prepared in this work were identified by X-ray diffraction using Bruker AXS Diffractomètre D8 Advance diffract meter using Cu-Kα radiation. XRD patterns were presented from $2\theta = 10°–60°$. Infrared spectra were performed on a FTIR Nicolet iS10 Thermo Fisher spectrometer using FTIR iTR. Thermogravimetric measurements were performed with TA Instruments "SDT Q600" combined to

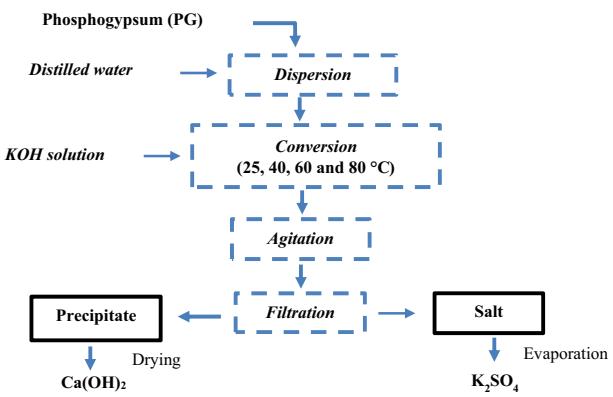

Fig. 1 Diagram of the procedure for converting PG

a mass spectrometer Hiden 0–200 uma. Small quantity of products was placed in an alumina crucible and heated from 20 to 900 °C at a speed of 5 °C min^{-1} under dry air flow of 100 mL min^{-1}. Also the obtained precipitate at optimal conditions was characterized at – 196 °C by physisorption of N_2 using Micrometrics ASAP2020, which is an automated volumetric apparatus. The specific surface area was calculated using Brunauer–Emmett–Teller (BET) model. Its morphology was observed by scanning electron microscopy X-ray analysis (SEM Environmental FEI Quanta 200). X-ray fluorescence was used to characterize major elements is an XRF spectrometer S4 PIONEER BRUKER aXS, which is equipped with an X-ray tube of 4 kW. Concentrations of trace elements were determined by inductively coupled plasma mass spectrometry (ICP-MS Model HP-4500) after acid digestion. Potassium and sodium concentrations are determined by flame photometer (FP JENWAY 500–731 Model PFP7). Measurements are made three times to make sure the determined values.

Results and discussion

The process consists of dispersing PG in a KOH solution using stoichiometric concentrations of 0.7–1.3 M of PG at ambient pressure and at various temperatures under constant magnetic agitation for 1 h. The basic reaction describing this process is:

$$CaSO_4 \cdot 2H_2O + 2KOH \rightarrow K_2SO_4 + Ca(OH)_2 + 2H_2O \quad (7)$$

This process leads to the PG dissolution and the precipitation of $Ca(OH)_2$ as whitish solid phase. After filtration, filtrate was evaporated to dryness in the oven, yielding transparent salts K_2SO_4. The maximum solubility of K_2SO_4 at the chosen temperatures of 25, 40, 60 and 80 °C correspond to the concentrations of 0.6, 0.8, 1 and 1.2 M, respectively. We cannot exceed the maximum temperature of 80 °C for the PG conversion. Otherwise, the gypsum can be transformed into plaster, which therefore becomes less reactive. According to reaction process, PG and K_2SO_4 concentrations are equals, so the mixtures studied in this work are 0.7, 0.9, 1.1 and 1.3 M at 25, 40, 60 and 80 °C, respectively, which are just after saturation concentrations at these temperatures.

Search for optimal conditions of concentration and temperature

For 0.7 M of PG, DRX pattern of obtained precipitate (Fig. 2a) corresponds mostly to portlandite $Ca(OH)_2$ (JCPDS N°: 01–076-0571) which exhibits an hexagonal structure. A very small amount of $CaCO_3$ (JCPDS N°: 01–072-1937) was detected. The presence of calcium carbonate results from carbonation when preparing the samples. It has rhombohedra structure. A low quantity of inert quartz (JCPDS N°: 00–033-1161) is also detected. It comes from impurities included in PG remaining inert and not attacked during this conversion and appears in solid XRD patterns. Existence of unreacted PG (JCPDS N°: 01–074-1433) show that the reaction is not complete even longer than four hours. In addition, syngenite (JCPDS N°: 00–028-0739) is detected, which crystallizes in monoclinic structure, it is a salt of calcium and potassium sulfate $(K_2Ca(SO_4)_2 \cdot H_2O)_2$ ($Kps = 3.54 \times 10^{-8}$ at 25 °C). The formation of syngenite is due to the oversaturation of the reaction medium by K_2SO_4 which reaches its maximum solubility of 0.6 M at 25 °C.

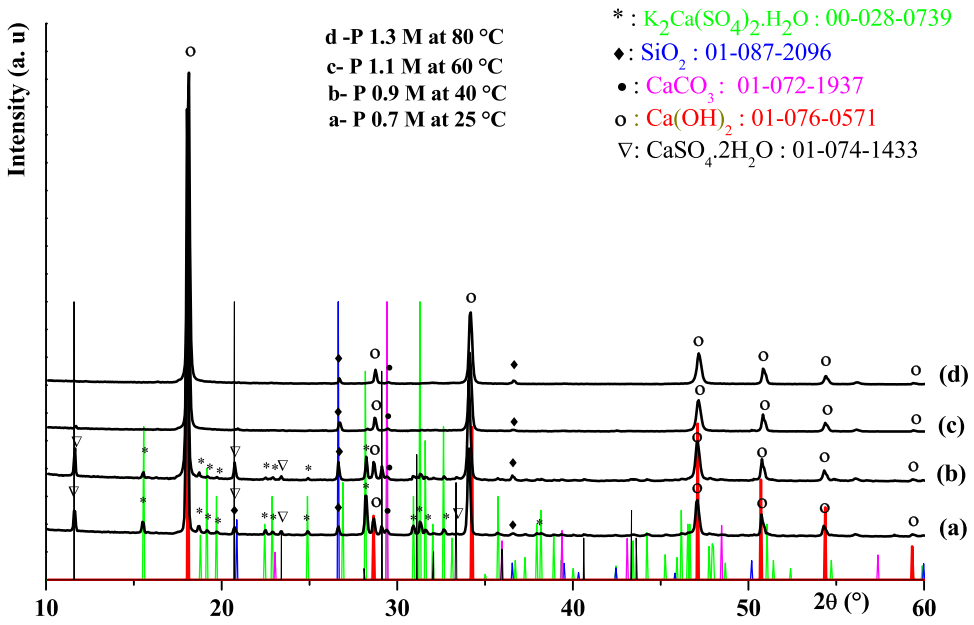

Fig. 2 XRD patterns of precipitates obtained at different temperatures

Thus, K_2SO_4 partially reacts with PG and forms syngenite according to the following reaction:

$$K_2SO_4 + CaSO_4 \cdot 2H_2O(s) + H_2O + K_2Ca(SO_4)_2 \cdot H_2O(s) \quad (8)$$

To prevent the formation of this parasitic phase of syngenite, we have studied the decomposition of PG at higher temperatures (40, 60 and 80 °C) which increases K_2SO_4 solubility and consequently push the reaction to higher concentrations of K_2SO_4.

XRD pattern of the precipitate corresponding to the concentration 0.9 M of PG at 40 °C (Fig. 2b) is similar to that of 0.7 M. The increase of the concentration to 0.9 M leads to $Ca(OH)_2$ and syngenite which appears also in the precipitate since the medium becomes over saturated by K_2SO_4 (reaction 8). In addition, the presence of a small amount of PG reveals that its decomposition is not complete in these conditions.

For the same purpose, we studied the decomposition of PG at 60 and at 80 °C. As before, we chose for each temperature concentrations after saturation of the medium by K_2SO_4. XRD patterns P 1.1 M-60 °C and P 1.3 M-80 °C (Fig. 2c, d) represent the obtained precipitates. These XRD patterns correspond to the formation of a major phase of portlandite $Ca(OH)_2$. This occurs even in media oversaturated by K_2SO_4. The absence of PG indicates that its decomposition is complete. Moreover, syngenite does not appear. Apparently, this competitive and parasitic phase is not stable at these temperatures.

Salts recovered from the filtrates under these optimal conditions are also characterized by XRD. Figure 3 shows DRX patterns of obtained salts. All filtrates (Fig. 3a–d) are well crystallized and confirm the formation of arkanite K_2SO_4 (JCPDS N°: 00–083-0682) with orthorhombic structure. A small amount of potassium carbonate K_2CO_3 (JCPDS N°: 00–001-1001) is observed in the XRD patterns corresponding to the concentrations 0.7 M and 0.9 M of PG at 25 °C and 40 °C, respectively (Fig. 3b). It is formed when Saturated PG react with saturated K_2SO_4 instead of KOH, this later react with atmospheric CO_2 to form K_2CO_3. Whereas recovered filtrates corresponding to the concentrations 1.1 M and 1.3 M of PG at 60 °C and 80 °C, respectively, correspond to arkanite K_2SO_4.

By combining XRD analyzes results of obtained precipitates and filtrates, it appears clear that increasing the temperature allowed the total PG conversion with high concentration and avoid the formation of syngenite at lower temperatures. The choice of 80 °C instead of 60 °C is very important because it will be possible to recover a filtrate more concentrated in K_2SO_4 (1.3 M instead of 1.1 M) which facilitates its recrystallization after cooling.

Therefore, the optimal conditions for the total conversion of PG by KOH to obtain a high concentration of K_2SO_4 are as follows: stoichiometric mixture using the concentration 1.3 M of PG during 1 h at 80 °C.

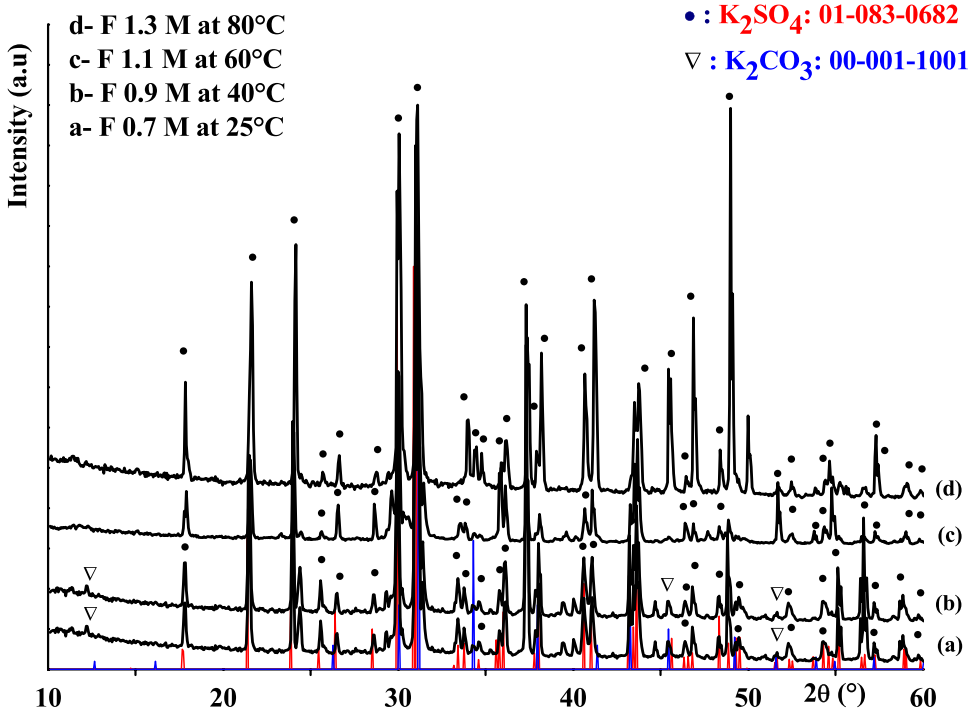

Fig. 3 XRD patterns of recovered salts at different temperatures

Infrared study

The products obtained by conversion of PG have also been identified by FTIR. The infrared spectrum of the PG sample is illustrated in Fig. 3 (PG). We can notice two asymmetric stretching bands at 1100 and 1004 cm^{-1} and two bending vibration bands at 666 and 596 cm^{-1} attributed to sulfate group SO_4^{2-}, it appears also the band at 837 cm^{-1}, it corresponds to HPO_4^{2-} which is syncrystallized with PG [27]. FTIR spectra evolution from 25 to 80 °C show a decrease of sulfate bands in obtained precipitates P 0.7 M-25 °C and P 0.9 M-40 °C (Fig. 4a, b). Sulfate bands are due to unreacted PG or syngenite formation. For spectra of precipitates P 1.1 M-60 °C and P 1.3 M-80 °C (Fig. 4c, d), characteristic bands corresponding to portlandite $Ca(OH)_2$ appear and those of sulfate disappear, whereas different vibration modes C–O of carbonate groups CO_3^{2-} are visible at 1417 and 872 cm^{-1} [28, 29]. The presence of calcium carbonate is explained by the following reaction:

$$CO_2 + Ca(OH)_2 \rightarrow H_2O + CaCO_3 \quad (9)$$

Moreover, we observed a band at 1055 cm^{-1} assigned to Si–O stretching mode of SiO_2 [13, 27].

The infrared spectra of obtained salts (Fig. 5) show similar characteristic bands of pure arkanite K_2SO_4 except for bands of carbonate group CO_3^{2-}. Table 1 summaries vibration band frequencies and their assignments for PG and obtained products at optimum conditions. From these results, we can notice that the conversion of PG waste is a valid means and permits to obtain a portlandite and an arkanite quite pure.

Raman study

The Raman spectra of PG and obtained products at optimum conditions are shown in Fig. 6. The principal vibrational modes of PG, precipitate P 1.3 M-80 °C and salt F 1.3 M-80 °C are assigned in Table 1.

In PG Raman spectrum, the strongest peak was found at 1011 cm^{-1} and was assigned to υ_{ss} symmetric stretch vibration mode of SO_4 tetrahedra. For pure gypsum, it appears at 1008 cm^{-1}. The other peaks, which are weaker, correspond also to SO_4 tetrahedra. The peak at 1139 cm^{-1} (1135 cm^{-1} in pure gypsum) corresponds to υ_3 antisymmetric stretch vibration mode, and peaks at 619 and 669 cm^{-1} (620 and 670 cm^{-1} in gypsum) are attributed to υ_4 antisymmetric bending vibration modes. PG shows for υ_2 symmetric bending of the SO_4 tetrahedra a doublet at 419 and 495 cm^{-1} (415 and 439 cm^{-1} in pure gypsum). Generally, the covalence of the bonds in a given structure as in the case of the ionic group SO_4^{2-} and its chemical environment cause it a systematic displacement of the Raman peaks.

In Raman spectrum of the salt F 1.3 M-80 °C, peaks observed at 1146 cm^{-1} and 1092 cm^{-1} (1137 cm^{-1} and 1096 cm^{-1} in K_2SO_4 crystal) were assigned to υ_3 asymmetric stretching vibration mode of SO_4 groups. Symmetric stretching υ_1 of SO_4 groups is assigned in the frequency 988 cm^{-1} (978 cm^{-1} in K_2SO_4 crystal). The peaks observed at frequencies 620 cm^{-1} and 453 cm^{-1} (448 cm^{-1} in K_2SO_4 crystal) were assigned to the asymmetric bending δ_4 of SO_4 groups. The two small peaks observed at 1108 and 1065 cm^{-1} correspond to the symmetric stretching vibration mode υ_1 of the CO_3^{2-}, which is degenerate. This degeneration of the vibration mode of

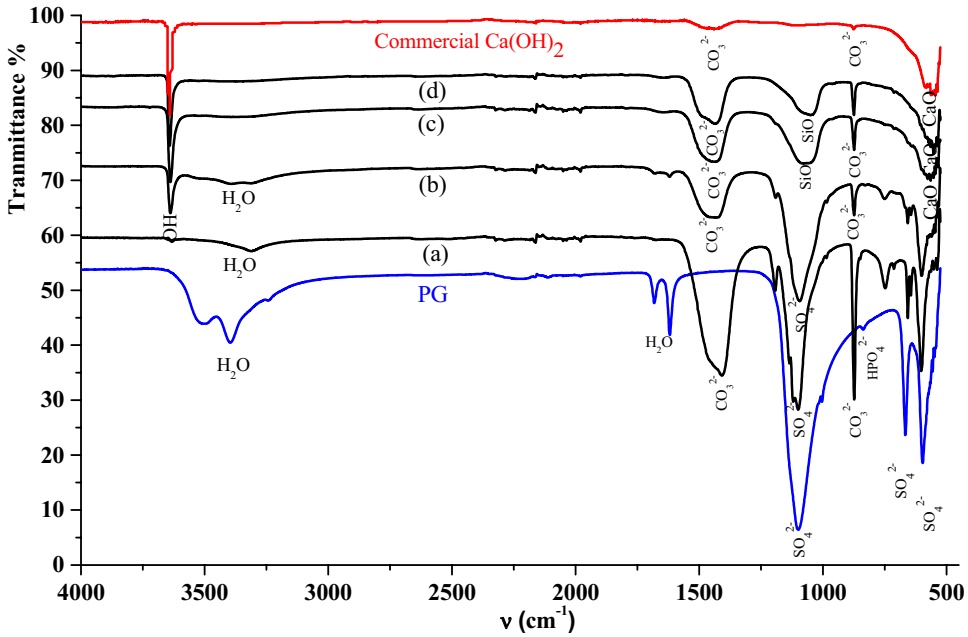

Fig. 4 FTIR Spectra of phosphogypsum (PG), precipitates P 0.7 M-25 °C (**a**), P 0.9 M-40 °C (**b**), P 1.1 M-60 °C (**c**), P 1.3 M-80 °C (**d**) and commercial $Ca(OH)_2$

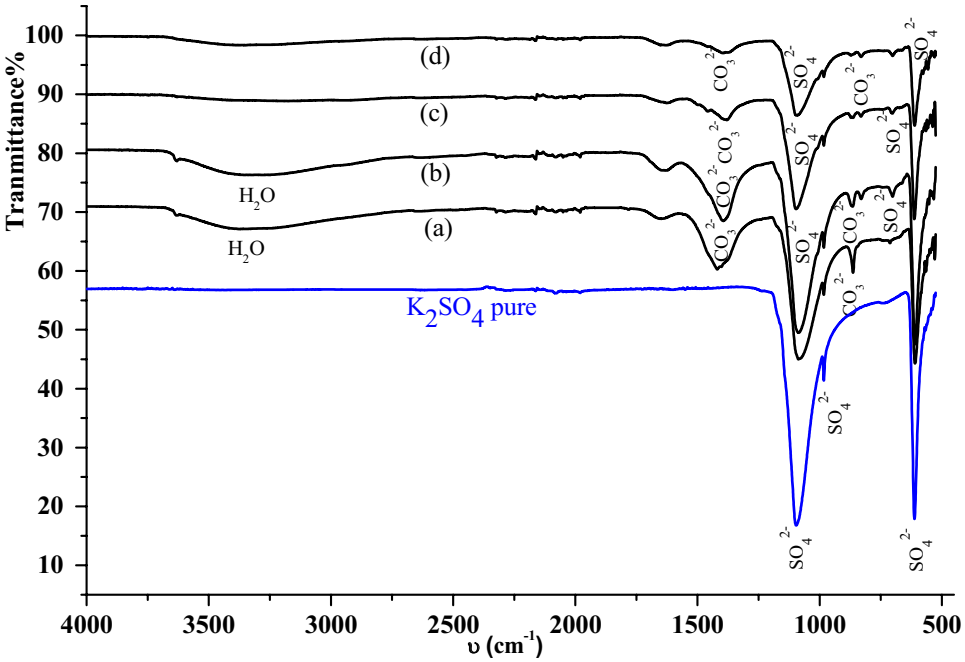

Fig. 5 FTIR Spectra of K_2SO_4 (PG) and salts F 0.7 M-25 °C (**a**), F 0.9 M-40 °C (**b**), F 1.1 M-60 °C (**c**), F 1.3 M-80 °C (**d**)

Table. 1 Infrared and RAMAN frequencies of PG, precipitate and salt synthetized at optimal conditions

Assignment		Wave number ν (cm^{-1})					
		PG		Precipitate		Salt	
		FTIR	RAMAN	FTIR	RAMAN	FTIR	RAMAN
H_2O	ν_3	3501–3396	–	3419	–	–	–
	δ_2	1682; 1619	–	–	–	–	–
	ν_T	–	520	–	–	–	–
OH	ν	–	–	3638	3600	–	
SO_4^{2-}	ν_3	1100	1140	–	–	1100	1146; 1092
	ν_1	1004	1012	–	–	982	988
	δ_4	666; 596	620; 670	–	–	673; 613	620; 453
	ν_2	–	420; 495	–	–	–	–
CO_3^{2-}	ν_3	–	–	1417	–	1423	–
	ν_2	–	–	872	–	855	–
	ν_1	–	–	–	–	–	1108; 1065
HPO_4^{2-}	ν	837	–	–	–	–	–
CaO	ν	–	–	553; 580	650	–	–
Si–O	ν	–	–	1055	–	–	–

υ_1 let's suppose the existence of two different symmetrical stretching modes in two types of sites for CO_3^{2-} ions [30].

In Raman spectrum of the precipitate P 1.3 M-80 °C, stretching vibration mode of Ca–O appears at 650 cm^{-1} in addition to a narrow peak observed at 3600 cm^{-1} typical of stretching vibration mode of OH of calcium hydroxide.

TGA-MS measurements under dry air atmosphere.

Thermal analyzes are useful for the determination of Ca $(OH)_2$ content because it is a relatively simple and fast technique compared to other methods. $Ca(OH)_2$ decomposes approximately at about 350 °C or 550 °C [31]. It depends on various factors, like quantity of the sample, the pressure in the

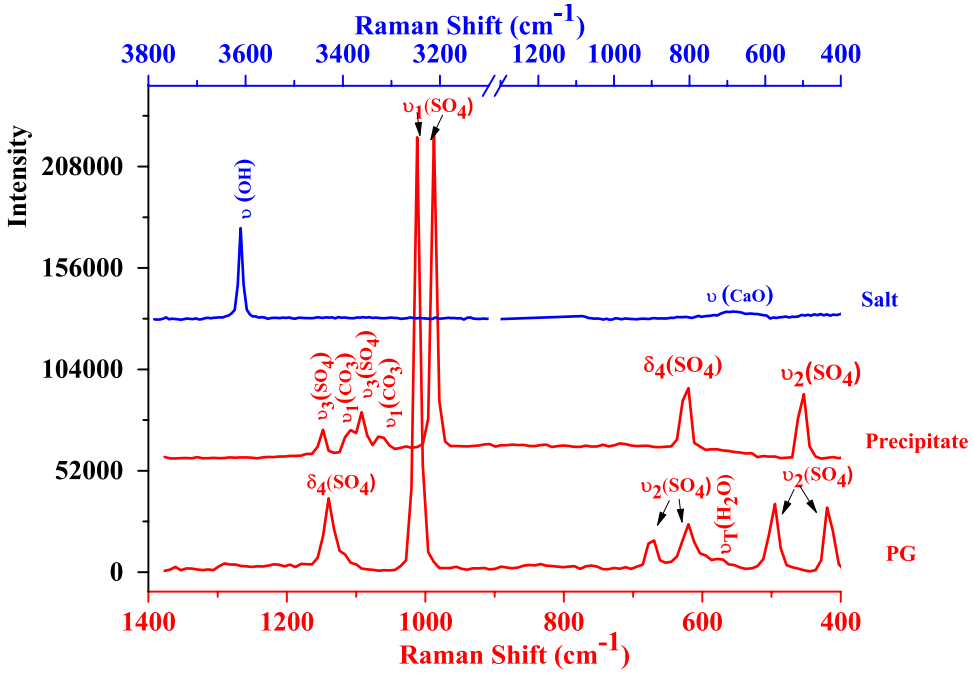

Fig. 6 Raman spectra of PG, precipitate P 1.3 M-80 °C and salt F 1.3 M-80 °C

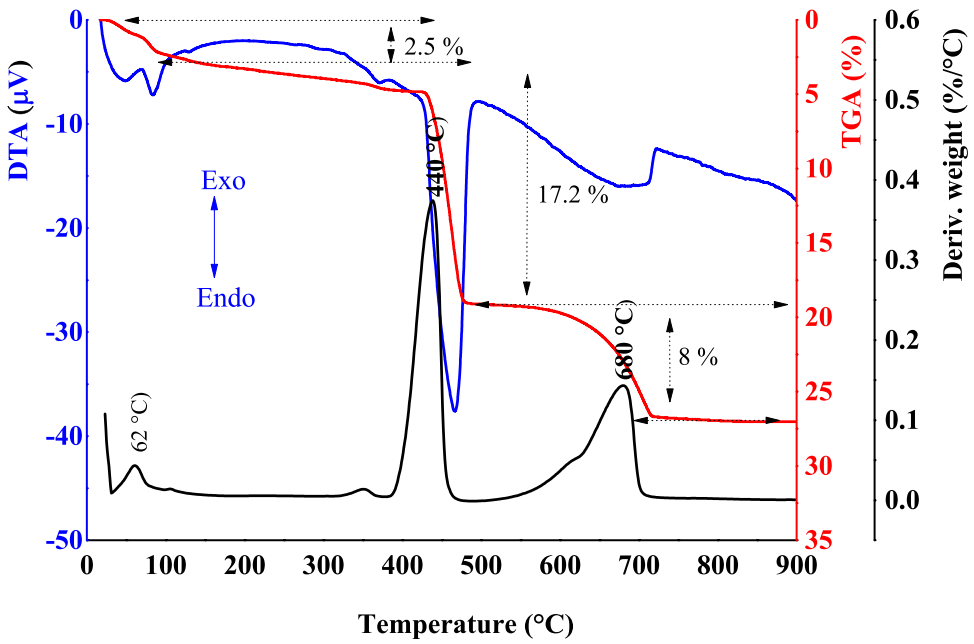

Fig. 7 DTA–TGA and derivative curves of the weight loss of precipitate P 1.3 M-80 °C

instrument and material fineness or crystallinity. The TGA, Deriv. weight and DTA curves of precipitate (P 1.3 M- 80 °C) are represented in Fig. 7. TGA exhibits two weight losses at 440 °C and 680 °C. Mass spectroscopy measurements (TGA-MS) indicate that there is elimination of water (m/e 18) and carbon dioxide (m/e 44). This evidences the following decomposition reactions:

$$Ca(OH)_2 \rightarrow CaO + H_2O \quad (m/e\ 18) \tag{10}$$

$$CaCO_3 \rightarrow CaO + CO_2 \quad (m/e\ 44) \tag{11}$$

The TGA results confirm that a certain quantity of calcium carbonate ($CaCO_3$) was produced as a result of the carbonation of $Ca(OH)_2$ along the sample preparation process. It is really difficult to perform all sample preparation operations (like, grinding, mixing or drying) in an atmosphere free of CO_2.The start of $CaCO_3$ decomposition begins after decomposition of $Ca(OH)_2$. The decomposition of $CaCO_3$

takes place over a much wider temperature range (500–700 °C). From data, we determine the temperatures of the beginning and the end of each decomposition then, we report the corresponding masses in equations below to determine $Ca(OH)_2$ and $CaCO_3$ contents.

$$\%\ Ca(OH)_2 = \frac{74}{18} \cdot \frac{m^P_{start} - m^P_{end}}{m^P_{start}} \cdot 100$$

$$\%\ CaCO_3 = \frac{100}{44} \cdot \frac{m^C_{start} - m^C_{end}}{m^P_{start}} \cdot 100$$

where m^P_{start}, m^P_{end}, m^C_{start} and m^C_{end} are masses (g) obtained by the TGA measurements at the start and at the end temperatures of $Ca(OH)_2$ and $CaCO_3$ decompositions, respectively.

According to the formulas above, the precipitate is composed of 70.82% of $Ca(OH)_2$ and 18.25% of $CaCO_3$. Pressler et al. mentioned that X-ray diffraction study methods usually give a lesser $CaCO_3$ value because it allows determining only its crystallized form [32].

The first weight losses bellow 200 °C is small (2.5%), and it is due to the removal of crystallized or adsorbed water of certain chemicals impurities like $MgSiF_6{\cdot}6H_2O$, $CaHPO_4{\cdot}2H_2O$, $CaFPO_3{\cdot}2H_2O$.

TGA curve of salt (F 1.3 M-80 °C) indicates a small weight loss of 1.2%, which justify that this salt is anhydrous (Fig. 8). For K_2SO_4 prepared by the evaporation method, Anooz et al. detected a weight loss 0.8% [33]. The endothermic peak observed on the DTA curve at 585 °C corresponds to a structural transformation of K_2SO_4 from orthorhombic (β) to hexagonal (α) form. This transition is observed at 587 °C by M. Miyake et al. for pure K_2SO_4 [34].

Particle size

Analysis by laser granulometry gives a curve (Fig. 9) from which we can visualize the grains distribution as well as the thickness of the sample. We note that there are practically no particles larger than 1000 µm and that 71% of the sample weight results from particle sizes in the range 37–250 µm. The granulometric distribution in the precipitate (P 1.3 M-80

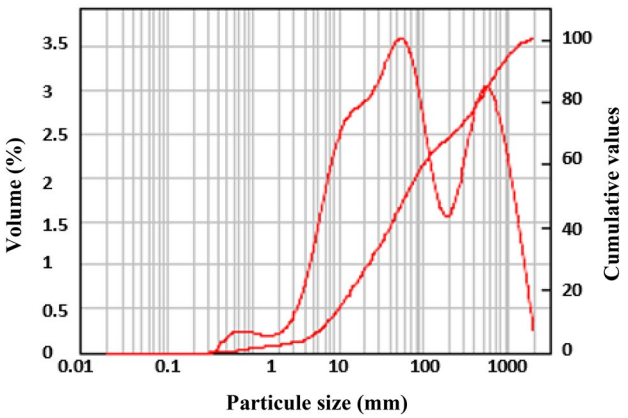

Fig. 9 Particle size distribution of precipitate P 1.3 M-80 °C

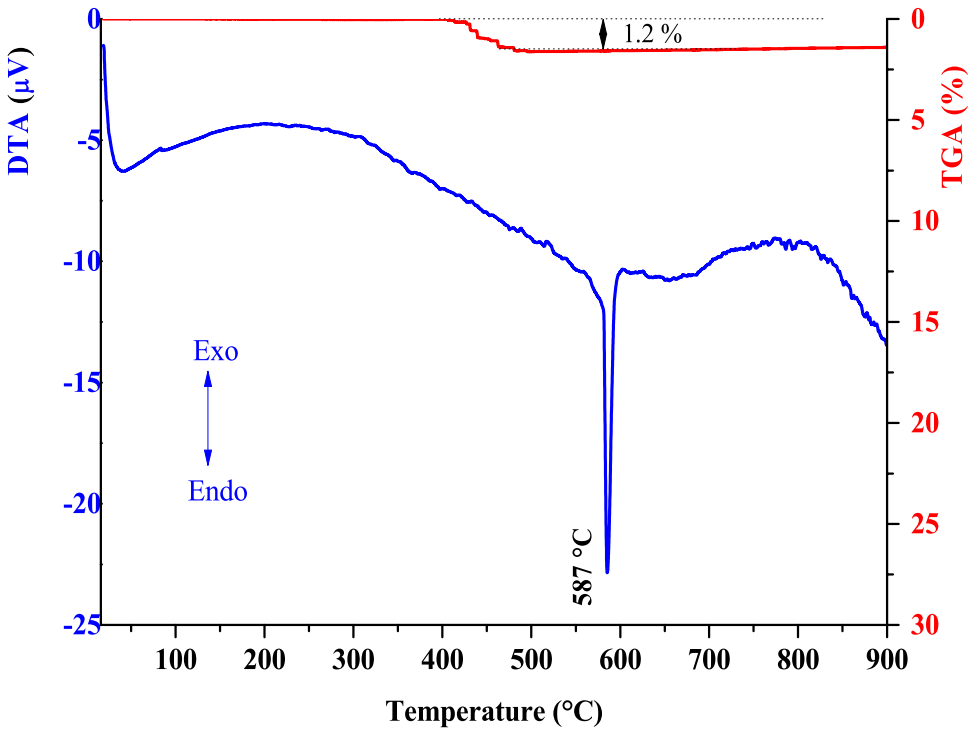

Fig. 8 DTA–TGA curves of salt F 1.3 M-80 °C

°C) exhibits two populations. The first one has a particle sizes around 75 µm in diameter. The second has grains of about 650 µm in diameter (Fig. 9).

Observation by scanning electron microscopy (SEM)

SEM technique investigates morphological structure PG and products synthesized synthetized at optimum conditions. Figure 10a illustrates that PG crystals form is tabular and their size varies from 5 to 30 µm.

Morphological structure of obtained precipitate (P 1.3 M-80 °C) indicates two distinctive shapes of particles. The first shape is predominant and slightly rounded. According to the XRD, portlandite is hexagonal, but the phenomenon of dissolution of $Ca(OH)_2$ gives it a rounded rather than hexagonal shape. The second form of minority crystals (as indicated in yellow zones in Fig. 10b) is attributed to calcite, which was also detected by XRD crystallizing in the rhombohedral structure. Similar observations have been cited by Regnault Olivier et al. in the experimental kinetic study of the carbonation of portlandite with CO_2 [35].

The obtained translucent salt F 1.3 M-80 °C recrystallized after the drying filtrate, was formed by macrocrystals of length between 3 to 6 mm and has the form of rods (Fig. 10c). This permits to get K_2SO_4 easily after recrystallization.

According to SEM–EDX (Fig. 10a′), we can say that PG particles are composed principally by Ca, S and O (gypsum) beside a low quantity of Si. The precipitate (P 1.3 M-80 °C) is formed essentially by Ca and O, the presence of Si, F and P is due to insoluble impurities remaining in the solid phase after filtration. The salt (F 1.3 M-80 °C) is manly composed by K, S and O. A presence of C is also detected.

BET measurement

By the nitrogen Adsorption- Desorption isotherm presented in Fig. 11, obtained precipitate (P 1.3 M-80 °C) develops a low BET surface area around 11 m^2/g and pore size diameter close to 14 nm which explain that the precipitate have a mesoporous property. This isotherm can be classified as type IV according to International Union of Pure and Applied Chemistry (IUPAC) classification. To explain this result, crystalline size is calculated by Scherer equation:

$$D(\text{Å}) = \frac{\lambda}{\beta \cos(\theta)}.$$

where D(Å): the crystallite size, λ: Cu-Kα radiation (1.5418 Å), β: Full Wide at High Middle (FWHM). This value is corrected using LaB_6 standard. θ: The most intense peak position. The crystalline size calculated is 80 nm. This large crystallite size calculated is in agreement with the low surface area found by BET.

Chemical elements distribution

Chemical analysis results of the of precipitate and salt obtained from PG conversion by KOH at 80 °C using 1.3 M of PG during one hour, are collected in Table 2. They give an idea about the existing impurities and their distribution between the powder and the salt during the total conversion reaction.

The process of PG conversion can be followed through the major elements S, Ca and K. Agreeing to the XRD and XRF results, the majority of Ca was transported from PG to the precipitate. Furthermore, maximum of the S in the PG was found in the filtrate with K coming from potassium hydroxide. Other elements such as P, Si, F and Al were also completely transported to the portlandite. As regards the trace impurities initially contained in PG, most of these elements were also found to have been completely transferred to the precipitate.

The dissolution of phosphogypsum and precipitation of portlandite implies a loss of mass and, therefore, an increase effect in the concentration of contaminants. In the filtrate, most contaminants are in lower concentrations with some values close to or even below the detection limit. Previous studies that we have done show that the distribution of major and trace elements after PG conversion by K_2CO_3 is similar to our results [14].

Conclusion

The high amount of phosphogypsum waste generated by the fertilizer industry in Morocco, as well as the CO_2 emissions generated by the same industry make our work an attractive and environmentally friendly solution. The effect of temperature on phosphogypsum conversion was evidenced reacting a high concentration of phosphogypsum waste (1.3 M) with potassium hydroxide to produce portlandite $Ca(OH)_2$ and potassium sulfate K_2SO_4. At 80 °C, the conversion is complete since we were able to avoid the formation of syngenite phase which blocked this conversion reaction. In addition, the reaction becomes faster complete after only one hour.

Obtained portlandite can be used for CO_2 sequestration from the production plant and can be converted into calcium carbonate which is useful in cement industry and for the treatment of solutions with abnormally high acidity and metal concentrations like in regions of experiencing intense mining activity. Our results support the development of an economically viable carbon sequestration technology based on the reuse of this industrial waste.

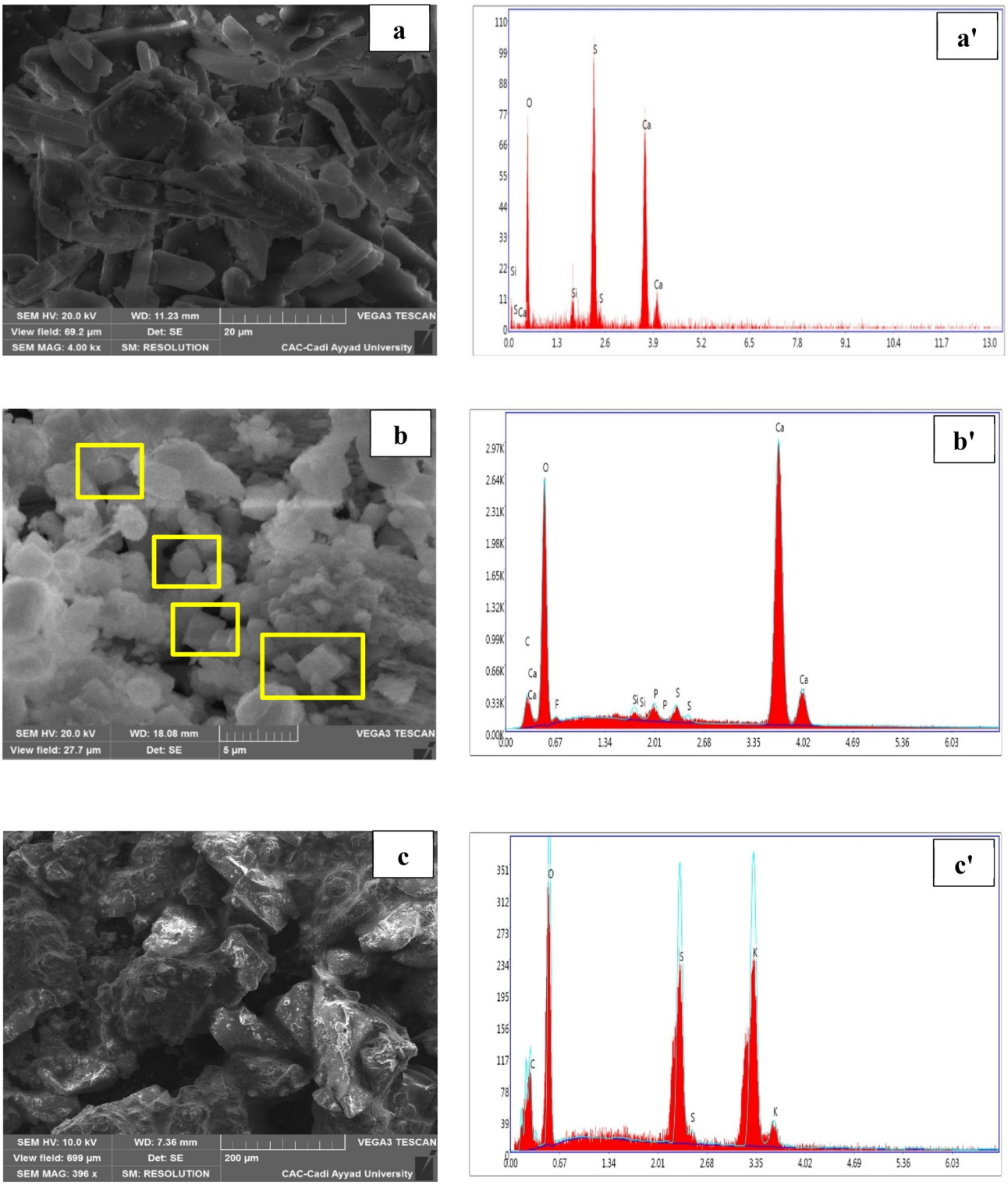

Fig. 10 SEM–EDX images PG, precipitate P 1.3 M-80 °C and salt F 1.3 M-80 °C

In addition, since the main impurities contained in the phosphogypsum are transferred into portlandite, the obtained potassium sulfate is high purity, which allows its marketing. The temperature chosen for the conversion reaction (80 °C) makes it possible to obtain a supersaturated filtrate of K_2SO_4, which facilitates its recrystallization by cooling at ambient temperature. This economical process permits to profit of about 500 $ per ton of PG converted,

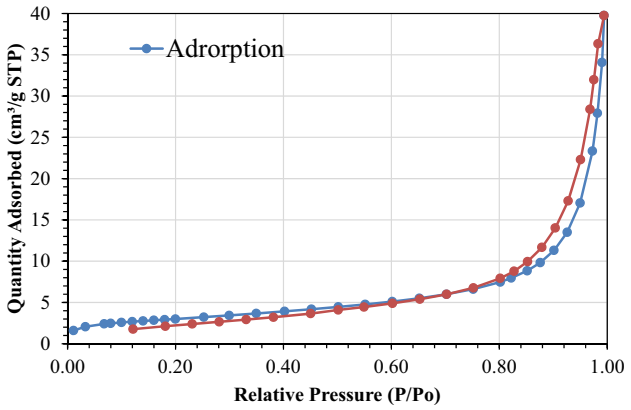

Fig. 11 Nitrogen adsorption–desorption isotherms of precipitate P 1.3 M-80 °C

Table 2 Major elements contents in wt% of PG, precipitate (P 1.3 M-80 °C) and salt (F 1.3 M-80 °C) analyzed by ICP

	PG	Precipitate (P 1.3 M-80 °C)	Salt (F 1.3 M-80 °C)
Major elements			
CaO	33.83	64.15	0.83
SO_3	42.52	3.24	43.49
K_2O	0.03(1)	3.84(1)	52.78(1)
Na_2O	0.08(1)	0.09(1)	0.22(1)
P_2O_5	0.19	0.4	0.002
SiO_2	0.28	0.47	0.23
F	0.59(2)	0.970(2)	0.077(2)
Al_2O_3	0.09	0.13	0.009
MgO	0.05	0.11	0.01
ZnO	0.04	0.47	0.03
SrO	0.08	0.07	0.007
CO_2	–	7.92(LOI)	–
H_2O	21.8(LOI)	18.38(LOI)	–
Trace elements			
As_2O_3	nd	nd	nd
Se_2O_3	nd	nd	nd
TiO_2	0.01	0.01	nd
Y_2O_3	0.02	0.03	nd
Cr_2O_3	0.02	0.04	0.02
ZrO_2	0.02	0.03	0.0002
PbO	0.01	0.01	nd
Fe_2O_3	0.01	0.01	0.002

(1)Flame spectrometer

(2)Ionometric method

(LOI)Loss-Of-Ignition

which can largely cover transport cost and the energy used during this process and does not require any difficult operation for recuperating these marketable products.

Declaration

Conflict of interest On behalf of all authors, the corresponding author states that there is no conflict of interest.

References

1. Rentería-Villalobos M, Vioque I, Mantero J, Manjón G (2010) Radiological, chemical and morphological characterizations of phosphate rock and phosphogypsum from phosphoric acid factories in SW Spain. J Hazard Mater 181:193–203. https://doi.org/10.1016/j.jhazmat.2010.04.116
2. Lu SQ, Lan PQ, Wu SF (2016) Preparation of nano-$CaCO_3$ from phosphogypsum by gas-liquid-solid reaction for CO_2 sorption. Ind Eng Chem Res 55:10172–10177. https://doi.org/10.1021/acs.iecr.6b02551
3. Elfadil S, Hamamouch N, Jaouad A et al (2020) The effect of phosphate flotation wastes and phosphogypsum on cattle manure compost quality and plant growth. J Mater Cycles Waste Manag 22:996–1005. https://doi.org/10.1007/s10163-020-00997-5
4. Karim AA, Kumar M, Mohapatra S et al (2019) Co-plasma processing of banana peduncle with phosphogypsum waste for production of lesser toxic potassium–sulfur rich biochar. J Mater Cycles Waste Manag 21:107–115. https://doi.org/10.1007/s10163-018-0769-7
5. Akin Altun I, Sert Y (2004) Utilization of weathered phosphogypsum as set retarder in Portland cement. Cem Concr Res 34:677–680. https://doi.org/10.1016/j.cemconres.2003.10.017
6. Kumar S (2003) Fly ash-lime-phosphogympsum hollow blocks for walls and partitions. Build Environ 38:291–295. https://doi.org/10.1016/S0360-1323(02)00068-9
7. Singh M (2002) Treating waste phosphogypsum for cement and plaster manufacture. Cem Concr Res 32:1033–1038. https://doi.org/10.1016/S0008-8846(02)00723-8
8. Mihara N, Kuchar D, Kojima Y, Matsuda H (2007) Reductive decomposition of waste gypsum with SiO_2, Al_2O_3, and Fe_2O_3 additives. J Mater Cycles Waste Manag 9:21–26. https://doi.org/10.1007/s10163-006-0167-4
9. Bouargane B, Marrouche A, El Issiouy S et al (2019) Recovery of $Ca(OH)_2$, $CaCO_3$, and Na_2SO_4 from Moroccan phosphogypsum waste. J Mater Cycles Waste Manag 21:1563–1571. https://doi.org/10.1007/s10163-019-00910-9
10. Ennaciri Y, Zdah I, El Alaoui-Belghiti H, Bettach M (2020) Characterization and purification of waste phosphogypsum to make it suitable for use in the plaster and the cement industry. Chem Eng Commun 207:382–392. https://doi.org/10.1080/00986445.2019.1599865
11. Ennaciri Y, Bettach M, El A-B, Jadida E (2020) Phosphogypsum conversion into calcium fluoride and sodium sulfate. Ann Chim Sci Matér 44:407–412
12. Ennaciri Y, Bettach M, El Alaoui-Belghiti H (2020) Recovery of nano-calcium fluoride and ammonium bisulphate from phosphogypsum waste. Int J Environ Stud 77:297–306. https://doi.org/10.1080/00207233.2020.1737426
13. Ennaciri Y, Bettach M (2018) Procedure to convert phosphogypsum waste into valuable products. Mater Manuf Process 33:1727–1733. https://doi.org/10.1080/10426914.2018.1476763
14. Ennaciri Y, El A-B, Bettach M (2019) Comparative study of K_2SO_4 production by wet conversion from phosphogypsum and synthetic gypsum. J Mater Res Technol 8:2586–2596. https://doi.org/10.1016/j.jmrt.2019.02.013
15. El Alaoui-Belghiti H, Bettach M, Zdah I, Ennaciri Y, Assaoui J, Zegzouti A (2020) Optimization of conditions to convert

phosphogypsum into $Ca(OH)_2$ and Na_2SO_4. Moroc J Chem 8:594–605
16. Mientka A, Grzmil B, Tomaszewska M (2008) Production of potassium sulfate from potassium hydrosulfate solutions using alcohols. Chem Pap 62:123–126. https://doi.org/10.2478/s11696-007-0088-2
17. Fernández-Lozano JA, Wint A (1997) Production of glaserite and potassium sulphate from gypsum and sylvinite catalysed by ammonia. Chem Eng J 67:1–7. https://doi.org/10.1016/S1385-8947(97)00015-6
18. Abu-Eishah SI, Bani-Kananeh AA, Allawzi MA (2000) K_2SO_4 production via the double decomposition reaction of KCl and phosphogypsum. Chem Eng J 76:197–207. https://doi.org/10.1016/S1385-8947(99)00158-8
19. Shen W, Gan G, Dong R et al (2012) Utilization of solidified phosphogypsum as Portland cement retarder. J Mater Cycles Waste Manag 14:228–233. https://doi.org/10.1007/s10163-012-0065-x
20. Murthy MS, Raghavendrachar P, Sriram SV (1986) Thermal decomposition of doped calcium hydroxide for chemical energy storage. Sol Energy 36:53–62. https://doi.org/10.1016/0038-092X(86)90060-5
21. Zhang F, Parker JC, Brooks SC et al (2010) Prediction of uranium and technetium sorption during titration of contaminated acidic groundwater. J Hazard Mater 178:42–48. https://doi.org/10.1016/j.jhazmat.2010.01.040
22. Gerdemann SJ, O'Connor WK, Dahlin DC et al (2007) Ex situ aqueous mineral carbonation. Environ Sci Technol 41:2587–2593. https://doi.org/10.1021/es0619253
23. Kirchofer A, Brandt A, Krevor S et al (2012) Impact of alkalinity sources on the life-cycle energy efficiency of mineral carbonation technologies. Energy Environ Sci 5:8631–8641. https://doi.org/10.1039/c2ee22180b
24. Kirchofer A, Becker A, Brandt A, Wilcox J (2013) CO_2 mitigation potential of mineral carbonation with industrial alkalinity sources in the United States. Environ Sci Technol 47:7548–7554. https://doi.org/10.1021/es4003982
25. El Alaoui-Belghiti H, Zdah I, Ennaciri Y et al (2021) Valorisation of phosphogypsum waste as K_2SO_4 fertiliser and portlandite $Ca(OH)_2$. Int J Environ Waste Manag 27:363–377
26. U.S. Geological Survey (2020) Mineral commodity summaries 2020: U.S. Geological Survey. https://doi.org/10.3133/mcs2020
27. Ennaciri Y, Bettach M, Cherrat A, Zegzouti A (2016) Conversion of phosphogypsum to sodium sulfate and calcium carbonate in aqueous solution. J Mater Environ Sci 7:1925–1933
28. Blesa MJ, Miranda JL, Moliner R (2003) Micro-FTIR study of the blend of humates with calcium hydroxide used to prepare smokeless fuel briquettes. Vib Spectrosc 33:31–35. https://doi.org/10.1016/S0924-2031(03)00089-4
29. Liu T, Zhu Y, Zhang X et al (2010) Synthesis and characterization of calcium hydroxide nanoparticles by hydrogen plasma-metal reaction method. Mater Lett 64:2575–2577. https://doi.org/10.1016/j.matlet.2010.08.050
30. Behrens G, Ubic R (2006) Spectroscopy letters : an international journal for rapid raman spectra of vateritic calcium carbonate. Spectrosc Lett 28:983–995. https://doi.org/10.1080/00387019508009934
31. El-Jazairi B, Illston JM (1977) A simultaneous semi-isothermal method of thermogravimetry and derivative thermogravimetry, and its application to cement pastes. Cem Concr Res 7:247–257. https://doi.org/10.1016/0008-8846(77)90086-2
32. Pressler EE, Brunauer S, Kantro DL, Weise CH (1961) Determination of the free calcium hydroxide contents of hydrated portland cements and calcium silicates. Anal Chem 33:877–882. https://doi.org/10.1021/ac60175a020
33. Anooz BS, Bertram R, Klimm D (2007) The solid state phase transformation of potassium sulfate. Solid State Commun 141:497–501. https://doi.org/10.1016/j.ssc.2006.12.008
34. Miyake M, Minato I, Iwai SI (1979) Thermal phase transition of potassium sulfate, K_2SO_4: a high temperature polarizing light microscopic study. Phys Chem Miner 4:307–315. https://doi.org/10.1007/BF00307534
35. Regnault O, Lagneau V, Schneider H (2009) Experimental measurement of portlandite carbonation kinetics with supercritical CO_2. Chem Geol 265:113–121. https://doi.org/10.1016/j.chemgeo.2009.03.019